

Non-Markovian Configurational Diffusion and Reaction Coordinates for Protein Folding

Steven S. Plotkin and Peter G. Wolynes

Department of Physics and School of Chemical Sciences, University of Illinois, Urbana, IL, 61801

(October 6, 2018)

Abstract

The non-Markovian nature of polymer motions is accounted for in folding kinetics, using frequency-dependent friction. Folding, like many other problems in the physics of disordered systems, involves barrier crossing on a correlated energy landscape. A variational transition state theory (VTST) that reduces to the usual Bryngelson-Wolynes Kramers approach when the non-Markovian aspects are neglected is used to obtain the rate, without making any assumptions regarding the size of the barrier, or the memory time of the friction. The transformation to collective variables dependent on the dynamics of the system allows the theory to address the controversial issue of what are “good” reaction coordinates for folding.

Typeset using REVTeX

According to the energy landscape theory [1], protein folding can be seen as a stochastic motion of a few collective coordinates describing protein conformation, on an average thermodynamic potential [2]. To first approximation this motion is Brownian, and the folding time can be computed from diffusive rate theory [3,4]. A good quantitative comparison between the analytical energy landscape theory and lattice simulations of smaller proteins has been made [3]; The diffusive behavior of the reaction coordinate's motion is approximate; in lattice simulations a fraction of the trajectories have *ballistic* crossings over the barrier, while others are quite diffusive [5], suggesting a wide range of time scales for the collective reaction coordinate. Non-Markovian dynamics, expected on a rugged energy landscape, will affect reaction rates when the time to cross the top of the barrier is comparable to the memory time of the fluctuating forces acting on the collective coordinate. Analysis of such situations for reactions in condensed phases has led to a number of good approximations for rates [6–9]. In our treatment we use variational transition-state theory (VTST) [8–10] to discuss how non-Markovian dynamics of the chain affects folding, and to address the question of what is the best reaction coordinate for folding. We apply our results to the motion of a heteropolymeric protein chain, but many of the same issues occur for kinetics in other disordered systems, for example the nucleation of a crystal from a glassy liquid. We first discuss the form of the effective frequency-dependent friction $\hat{\zeta}(\omega)$ for motion on a correlated energy landscape, specifically for a heteropolymer. Then we apply VTST to find corrections to the Kramers folding rate due to memory effects in $\hat{\zeta}(\omega)$, and anharmonicities in the potential.

Protein conformational motion can be mapped onto a generalized master equation, with escape rates from a statistical ensemble of configurations given in terms of a waiting time distribution $P_Q(\tau, \tilde{T})$ [1]. The configurational states may be grouped together in strata with a common value of their similarity to the native conformation, which is an approximate reaction coordinate for folding. This is often taken to be Q [11,5], the fraction of native contacts, but other choices are possible. Finding a “best” reaction coordinate is currently of great interest [5,12–14]. By projecting onto this coordinate, a diffusion equation for its probability distribution is obtained with a frequency-dependent diffusion coefficient [1]. Correspondingly, the coordinate's motion can be characterized by an overdamped generalized Langevin equation (GLE): $-dF(Q)/dQ - \int_0^t d\tau \zeta_Q(t-\tau, T) \dot{Q}(\tau) + \xi(t) = 0$, with a frequency-dependent friction coefficient $\hat{\zeta}_Q(\omega, T) = k_B T / \widehat{D}_Q(\omega)$ satisfying $\langle \xi(t) \xi(t') \rangle = T \zeta_Q(t-t', T)$.

The GLE implies that Q responds linearly to fluctuations in the other coordinates of the polymer chain apart from the nonlinearity inherent in the thermodynamic potential for Q . This should be a good approximation if many individual configurational states of the polymer chain are sampled for each value of Q , as expected above the glass transition temperature of the stratum at Q . $\hat{\zeta}_Q(\omega, T)$ is given by averaging over $P_Q(\tau, T)$ as $\hat{\zeta}_Q(\omega, T) = \lambda_Q \langle \tau / (1 + \omega\tau) \rangle / \langle 1 / (1 + \omega\tau) \rangle$ or $\lambda_Q \mathcal{L}_t \langle e^{-t/\tau} \rangle / \mathcal{L}_t \frac{d}{dt} \langle e^{-t/\tau} \rangle$ where \mathcal{L}_t is the Laplace transform. The conformational motion distance scale is set by $\lambda_Q \equiv 2k_B T / (\Delta Q^2 \gamma_Q)$, where ΔQ is the step size and γ_Q is the probability a jump changes Q . $P_Q(\tau, T)$ on a *correlated* energy landscape is obtained by first defining a local progress coordinate q as similarity to the *given* trap state, so the typical rate of escape [15] involves the calculation of the free energy barrier $(F_Q(q^\ddagger) - F_Q(1))$ for motion to states having native similarity near to Q , assuming the elementary moves are sufficiently local. A bilinear approximation to the entropic part of $F_Q(q)$ can be used [15], since contacts formed at small q , i.e. for a more weakly constrained polymer, cost more entropy than for a strongly constrained one at high q . The escape time

$\propto \exp(\Delta F^\dagger/T)$ depends on 2 parameters: 1.) The reduced temperature $\tilde{T} = T/T_G$, where $T_G = (\Delta E_Q^2/2S_Q)^{1/2}$ is the glass temperature for the Q stratum. S_Q is the configurational entropy at Q while $\Delta E_Q^2 = (1-Q)(\Delta E_M^2 + Q\Delta E_N^2)$ is the energetic variance of the states in terms of the variance of native (N) and non-native (M) contacts, and 2.) The reduced energy of the trapped state $\tilde{E} = E/E_{GS}$, where $E_{GS} = -(2S_Q\Delta E_Q^2)^{1/2}$ is the ground state energy of the ensemble of states at Q . The escape time from a trap with energy \tilde{E} , $\tau_Q(\tilde{E}, \tilde{T})$, is given by $\tau_o \exp[S_Q(1-q^\dagger)(2\tilde{E}/\tilde{T} - 1/\alpha^\dagger - 1/\tilde{T}^2)\theta_r]$. Here q^\dagger is the location of the barrier peak, and $\alpha^\dagger = (1-q^\dagger)S_Q/S^\dagger$, where S^\dagger is the fraction of S_Q at the barrier peak (for the 64-mer $q^\dagger \cong 0.3$ and $\alpha^\dagger \cong 1.6$, see fig. 4-9 of [15]). For states with $\tilde{E} < \tilde{E}_A(\tilde{T})$ or when $\tilde{T} > \tilde{T}_A(\tilde{E})$ (determined by setting the barrier to zero), escape becomes downhill with short life-times of roughly the Rouse-Zimm time(s) $\simeq \tau_o$, hence $\theta_r = \theta(\tilde{E} - \tilde{E}_A(\tilde{T}))\theta(\tilde{T}_A(\tilde{E}) - \tilde{T})$ in the exponent. At $\tilde{T} = 1$ where the system is frozen into one of a few ground states ($\tilde{E} = 1$), and the typical escape time is $\tau_Q(1, 1) = \tau_o \exp[S_Q(1-q^\dagger)(1-1/\alpha^\dagger)] \cong \tau_o \exp(0.27 S_Q^{(64)})$. Correlations lower the free energy barrier to correspond to roughly 1/4 the total configurational entropy [15], as opposed to the full entropy as in uncorrelated landscapes. The distribution of occupied state energies \tilde{E} at temperature \tilde{T} is a Boltzmann weighted gaussian: $P_Q(\tilde{E}, \tilde{T}) \sim \exp[-S_Q(\tilde{E} - 1/\tilde{T})^2]$. Reflecting this, the distribution of escape times is easily calculated as $P_Q(\tau, \tilde{T}) = \int_{-1}^1 d\tilde{E} P_Q(\tilde{E}, \tilde{T})\delta[\tau - \tau_Q(\tilde{E}, \tilde{T})] = P_Q^{B-L} + P_Q^B$. Apart from barrier-less escapes with $P_Q^{B-L}(\tau, \tilde{T}) = \Delta(\tilde{T})\delta(\tau - \tau_o)$, this yields essentially a log-normal distribution:

$$P_Q^B(\tau, \tilde{T}) = \theta_B \frac{\tilde{T}A}{2S(1-q^\dagger)\tau} \frac{1}{e} \exp\left[-\frac{s}{4} \left[\frac{\tilde{T} \ln(\tau/\tau_o)}{s(1-q^\dagger)} - \frac{1}{\tilde{T}} + \frac{\tilde{T}}{\alpha^\dagger} \right]^2\right]$$

where $\theta_B = \theta(\tilde{T}_A(1) - \tilde{T})\theta(\tau - \tau_o)\theta(\tau_Q(1, \tilde{T}) - \tau)$, $S \equiv S_Q$, and $A = A_Q(\tilde{T})$ is the normalization constant of $P_Q(\tilde{E}, \tilde{T})$, while $\Delta = \Delta(\tilde{T})$ is the weight for fast escapes from states without barriers.

The above analysis applies at temperatures higher than the thermodynamic glass transition temperature T_G (but below the activation temperature T_A , where escape from all occupied states is barrier-less). At or below T_G the temperature independent distribution of state energies becomes $P(E) \sim \exp(E/T_G)$. Arrhenius-like escape from states yields the distribution of escape times $P(E(\tau))/\left|\frac{d\tau}{dE}\right| \sim \tau^{-(1+T/T_G)}$, giving stretched exponential relaxations [16,17]. In this regime the assumed linearity of Q dynamics is questionable however.

Evaluating $\widehat{D}_Q(\omega, \tilde{T})$ or $\widehat{\zeta}_Q(\omega, \tilde{T})$ above T_G , note that $\langle e^{-t/\tau} \rangle \sim \int_{z_L}^{z_U} dz e^{-Sz^2} \exp[-b\frac{t}{\tau_o} e^{-c_2 Sz}]$ (where $c_2 = 2(1-q^\dagger)/\tilde{T}$, and $b = \exp[S(1-q^\dagger)(1/\alpha^\dagger - 1/\tilde{T}^2)]$) is reminiscent of the after-effect function $f(bt/\tau_o, c_2/\sqrt{S})$ used for non-exponential decay in glasses [18]. But for the mesoscopic systems relevant to folding ($N \lesssim 100$), a better approximation is to linearize the gaussian term on the range $(z_L, z_U) = (\tilde{T}/2\alpha^\dagger - 1/2\tilde{T}, 1 - 1/\tilde{T})$, yielding a closed form expression for the friction

$$\widehat{\zeta}_Q(\omega, \tilde{T}) = \lambda_Q \frac{\frac{\Delta}{1+\omega} + \frac{F}{1-c} [f^{c-1} {}_2F_1(1, 1-c, 2-c, -\omega/f) - {}_2F_1(1, 1-c, 2-c, -\omega)]}{\frac{\Delta}{1+\omega} + \frac{F}{c} [{}_2F_1(1, -c, 1-c, -\omega) - f^c {}_2F_1(1, -c, 1-c, -\omega/f)]} \quad (1)$$

where ${}_2F_1$ is the hypergeometric function, ω is in units of $1/\tau_o$, $F = Ae^{S z_M^2}/c_2 b^c S$, $c = 2z_M/c_2$, $f = \tau_o/\tau_Q(1, \tilde{T}) < 1$, and $z_M = (z_U + z_L)/2$. The corresponding diffusion coefficient $\widehat{D}_Q(\omega, \tilde{T}) = k_B T/\widehat{\zeta}_Q(\omega, \tilde{T})$ is plotted in fig. 1.

Non-Markovian rate theory [8] proceeds by recognizing that the GLE is equivalent to a particle bilinearly coupled to a bath of oscillators [19] with an effective Hamiltonian $\mathcal{H} = p_Q^2/2 + F(Q) + \frac{1}{2} \sum_j [p_{x_j}^2 + (\omega_j x_j - c_j Q/\omega_j)^2]$ with $\zeta(t) = \sum_j (c_j^2/\omega_j^2) \cos(\omega_j t)$. These additional collective modes describe the dynamics of \dot{Q} fluctuations within linear response. Rather than dealing with non-Markovian dynamics of Q we can study the dynamics of this equivalent many-dimensional system without memory. When a single barrier exists in $F(Q)$ it makes sense to use multidimensional transition state theory. If the barrier is large and its parabolic part dominates, \mathcal{H} is quadratic and may be diagonalized by a normal mode transformation, which singles out as a reaction coordinate an unstable mode ρ with imaginary frequency $i\lambda^\ddagger$ given by the solution of $\lambda^\ddagger \widehat{\zeta}_{Q^\ddagger}(\lambda^\ddagger, \tilde{T}) = m\omega^{\ddagger 2} = |\partial^2 F(Q)/\partial Q^2|_{Q^\ddagger}$. This frequency is identical to the (overdamped) Grote-Hynes reactive frequency [6]. The effect of friction is to leave the barrier height unchanged, but to rotate the reaction coordinate to a different direction in configuration space. When the friction has no memory and the Q motion is purely diffusion, the reactive frequency is that of an overdamped inverted harmonic oscillator corresponding to the Kramers prefactor in the rate. For a general $F(Q)$ we can separate the quadratic part from the anharmonic part of F . Then in the normal coordinates at the saddle point $\mathcal{H} = \frac{1}{2}[p_\rho^2 - \lambda^{\ddagger 2} \rho^2 + \sum_j (p_{y_j}^2 + \lambda_j^2 y_j^2)] + F_1(u_{oo}\rho + \sum_j u_{jo}y_j)$. The coefficients u_{jo} are elements of the orthogonal normal-mode transformation such that $q \equiv Q - Q^\ddagger = u_{oo}\rho + \sum_j u_{jo}y_j$ (u_{oo} is given in terms of the friction kernel as $u_{oo}^2 = 1/[\widehat{\zeta}_{Q^\ddagger}(\lambda^\ddagger, \tilde{T})/\lambda^\ddagger + \partial \widehat{\zeta}_{Q^\ddagger}(s, \tilde{T})/\partial s|_{s=\lambda^\ddagger}]$). In addition to the Grote-Hynes coordinate ρ one can define a residual collective bath coordinate $\sigma \equiv (1 - u_{oo})^{-1/2} \sum_j u_{jo}y_j \equiv (1/u_1) \sum_j u_{jo}y_j$, which appears in the anharmonic part of the potential. The effects of dynamic friction, reflected by re-crossings in the Q coordinate, are in fact accounted for by ballistic motion across a new *thermodynamically* determined dividing surface involving a 2-D potential in (ρ, σ) [8]. The equilibrium flux across any dividing surface written in these new coordinates is

$$\Gamma = \frac{\int dp_\rho d\rho dp_\sigma d\sigma \delta(f) (\nabla f \cdot \mathbf{p}) \theta(\nabla f \cdot \mathbf{p}) e^{-\beta \mathcal{H}^\ddagger}}{\int dp_\rho d\rho dp_\sigma d\sigma e^{-\beta \mathcal{H}^\ddagger}}$$

Here $f = \rho - g(\sigma)$ serves as a new progress coordinate. $f = 0$ determines a dividing surface between reactants and products, the factor $\delta(f)$ localizes the integration to that surface, while $\nabla f \cdot \mathbf{p} = p_\rho \partial f / \partial \rho + p_\sigma \partial f / \partial \sigma$ is the flux density across the surface. The reduced Hamiltonian depends only on two coordinates ρ and σ : $\mathcal{H}^\ddagger = \frac{1}{2}[p_\rho^2 + p_\sigma^2 - \lambda^{\ddagger 2} \rho^2 + \Omega^2 \sigma^2] + F_1(u_{oo}\rho + u_1\sigma)$, with a collective bath frequency $\Omega^2 = u_1^2/(u_{oo}^2/\lambda^{\ddagger 2} - 1/\omega^{\ddagger 2})$. Carrying out the integrations, the rate can be written as a correction to the Grote-Hynes rate: $\Gamma = P(\lambda^\ddagger/\omega^\ddagger)\Gamma_0$. $\Gamma_0 = (\omega_o/2\pi) \exp(-\beta F^\ddagger)$ is the TST rate, while $\lambda^\ddagger/\omega^\ddagger$ is the G-H transmission factor. The additional correction to the G-H prefactor is given by a quadrature:

$$P = \left(\frac{\beta \Omega^2}{2\pi}\right)^{1/2} \int_{-\infty}^{\infty} d\sigma \sqrt{1 + \left(\frac{dg(\sigma)}{d\sigma}\right)^2} \exp(-\beta E[g]) .$$

Here $E[g] = \frac{1}{2}(\Omega^2 \sigma^2 - \lambda^{\ddagger 2} g(\sigma)^2) + F_1(u_{oo}g(\sigma) + u_1\sigma)$. If F_1 vanishes, the potential is parabolic, and variational minimization of the rate yields $f = \rho$ as the progress coordinate and $q = u_1\sigma \cong \sigma$ as the ideal dividing surface. The transition state position is coupled strongly to the bath mode, but the correction gives $P = 1$, reproducing the G-H rate $\Gamma = (\lambda^\ddagger/\omega^\ddagger)\Gamma_0$. For systems with large barriers $\gtrsim 10k_B T$, the parabolic approximation discussed above is

highly accurate but we can find corrections to it by finding a more general *planar* dividing surface $f = u_{oo}\rho + \sum_j u_{oj}y_j - \rho_o = 0$ (where ρ_o is the distance of the dividing surface from the barrier peak) oriented such that the TST rate is minimized. Using the variational framework developed in [9] along with the correlated landscape theory of $\hat{\zeta}_Q(\omega, \tilde{T})$, we find corrections to the GH rate at conditions of equilibrium between the folded and molten globule states (at T_F), see fig. 2. The optimal barrier location ρ_o (see inset A) is little different from the naive choice of the free energy maximum, for the 64-mer. The rate enhancement over the Kramers result has a peak at intermediate T_F/T_G due to the larger relative frequency dispersion of the diffusion coefficient at intermediate temperatures. For systems this large, the planar dividing surface assumption is accurate to within 5%.

For a 27-mer imitating a small protein at $T_F \cong 1.6T_G$, we can use the simulated auto-correlation function of Q , $c(t)$ (see fig. 9 of [3]), to determine $\hat{\zeta}(\omega)$: $\hat{\zeta}(\omega) = F''(Q^\ddagger)/(1/\hat{c}(\omega) - \omega)$. Here $\hat{c}(\omega) = \mathcal{L}_t c(t)$. For the 27-mer at T_F , the potential is very anharmonic. A planar dividing surface is no longer optimal. For such low barriers, minimizing the flux through the TST surface can be carried out using the calculus of variations as done by Miller [20] and Pollak [10]. Finding the stationary point of the rate for arbitrary variations of the dividing surface functional $\delta g(\sigma)$ yields a differential equation for $g(\sigma)$: $g''/(1 + g'^2) = \beta(g'\partial E[g]/\partial\sigma - \partial E[g]/\partial g)$. Treating g and σ as parametrized variables in terms of an independent parameter t (such that $g' = \dot{g}/\dot{\sigma}$, and setting the first integral $\frac{1}{2}(\dot{g}^2 + \dot{\sigma}^2) \equiv E_o - V_\beta$) recasts this variational equation into Hamilton's equations of motion for g and σ on an effective temperature dependent potential $V_\beta = -(1/2\beta) \exp(-2\beta E[g])$ at total energy $\frac{1}{2}(p_g^2 + p_\sigma^2) + V_\beta = 0$. The optimal dividing surface is a classical periodic trajectory on V_β with infinite period, that divides the (ρ, σ) space into reactants and products. The correction P is given in terms of the action along this optimal trajectory: $P = (\beta^2 \Omega^2 / 2\pi)^{1/2} \int ds \sqrt{-2V_\beta}$ where ds is arc-length along the trajectory. The optimal dividing surface for the 27-mer is plotted on the potential $E(\rho, \sigma)$ in fig. 3. The correction $P \cong 0.85$. The rate is moderately reduced from the G-H value of $1.57 k^{\text{KR}}$, giving $k = 1.33 k^{\text{KR}}$ for the corrected rate, in closer agreement with the naive Kramers value. While the Kramers approximation made in [3,4] is numerically quite accurate, the optimal dividing surface shows the transition region is quite spread out in the coordinate Q . By finding the optimal dividing surface, VTST seeks that coordinate which behaves most ballistically. Including the Q dependence of $\hat{\zeta}$ at higher nativeness may explain some of the discrepancy between simulations and rate calculations [3].

The present analysis can easily be generalized to include ordering along additional collective coordinates, as for example the total density of contacts, which is often important if collapse is not fast [21]. Potentially interesting effects may arise in such scenarios due to anisotropic friction [9], and are a topic of future work. The methods presented here are general, and also apply to other condensed matter systems with rugged landscapes, e.g. glasses and clusters. Nonlinear couplings between the system and bath may also be treated; This may allow explicit treatments of the deep traps in the glassy regime.

FIGURES

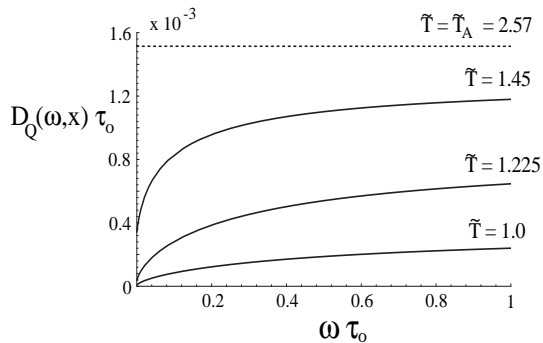


FIG. 1. $\tau_o \widehat{D}_{Q^\ddagger}(\omega, \tilde{T})$ for 64-mer near the transition state $Q^\ddagger \approx 0.3$, as a function of frequency (in units of τ_o), at several temperatures between the thermodynamic glass temperature and kinetic (activated) glass temperature. There is a rapid increase from the zero frequency value $\widehat{D}_Q(0, \tilde{T})$ dependent on the typical escape time, to a higher asymptotic value depending on how many of the states are untrapped and have short lifetimes at that temperature. The dispersion in the values of the diffusion is thus maximum at intermediate values of temperature. The largest values of the diffusion constant are set by $\sigma_Q \equiv k_B T / \lambda_Q$, and at \tilde{T}_A , $\widehat{D}_{Q^\ddagger}(\omega, \tilde{T}_A) = \sigma_Q = \Delta Q^2 \gamma_Q / 2\tau_o \approx 0.0015 / \tau_o$ for the 64-mer.

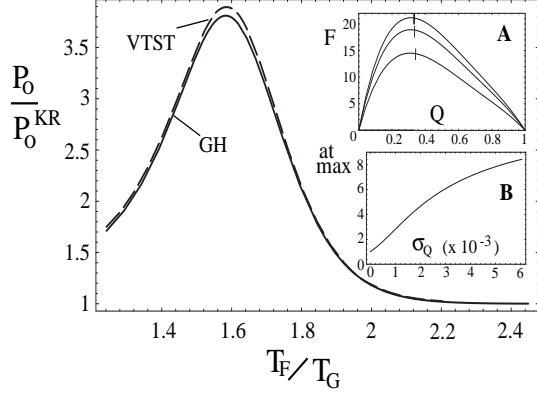


FIG. 2.

(solid line) Ratio of the Grote-Hynes rate to the Kramers rate, as a function of T_F/T_G . **(dashed line)** VTST rate enhancement including anharmonic effects of a finite size barrier. The effect here is small, however larger effects are seen for shorter polymers (see text). The system is a 64-mer at folding equilibrium. The variance of interaction energies is varied, so that the temperature ratio T_F/T_G varies ($T_F/T_G = \sqrt{\eta} + \sqrt{\eta - 1}$, with $\eta = E_N^2/2S_o\Delta E_M^2$, where E_N is the native state energy, and S_o is total entropy). The rate closely follows the G-H result $k^{\text{GH}}/k^{\text{KR}} = \hat{\zeta}_{Q^\ddagger}(0, \tilde{T})/\hat{\zeta}_{Q^\ddagger}(\lambda^{\text{GH}}, \tilde{T})$. **(Inset A)** Thermodynamic potentials vs. Q . For more rugged landscapes the barrier is flatter, and this reduces the prefactor to the rate since there are more recrossings. The T_F/T_G values are 2.45, 1.84, and 1.24 in order of decreasing barrier size. The small vertical bars near the barrier peak are where the VTST dividing surfaces cross the coordinate Q . **(Inset B)** Enhancement of the rate at the maximum value of 3.8 at $T_F/T_G \approx 1.6$ by allowing the prefactor $\lambda_Q \equiv k_B T/\sigma_Q$ in $\hat{D}(\lambda^{\text{GH}}, \tilde{T})$ to vary ($\sigma_Q \approx 0.0015$ is the original value).

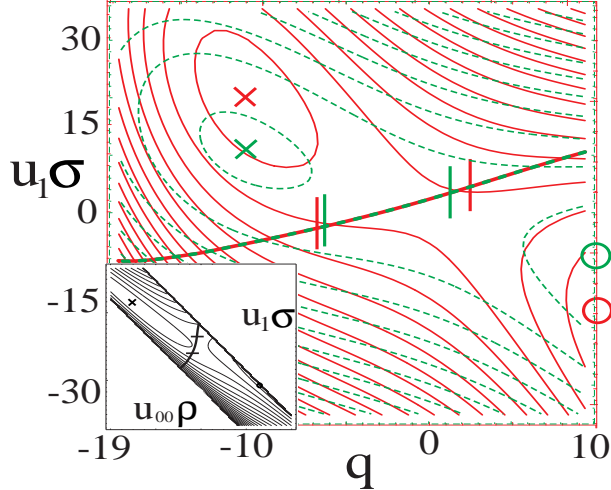


FIG. 3. (Color) Potential surface $E(q, u_1\sigma)$ (red) and in the normal coordinates $(u_{00}\rho, u_1\sigma)$ (inset), along with the variational dividing surface which minimizes the TST flux (heavy line). Contours are drawn at intervals of about $2k_B T$. The potential in the Markovian case (dashed green), with the corresponding Kramers rate, is further skewed with respect to the dividing surface, indicating paths in this case are even more diffusive. **X** marks the position of the molten globule minimum, and **O** the native minimum. The short vertical lines (and horizontal lines in inset) bound a region of $\approx 70\%$ of the total flux across the dividing surface. In $(q, u_1\sigma)$ space there is flux over a wide range of q values, $\Delta q / (q_{native} - q_{mg}) \approx 0.44$, so that the transition state theory that reproduces the multiple crossing physics in Kramers theory does not have a well defined value of q^\ddagger . However in $(u_{00}\rho, u_1\sigma)$ space the TST surface tends towards orthogonality to the reaction coordinate $u_{00}\rho$: $\Delta\rho / (\rho_{native} - \rho_{mg}) \approx 0.04$, indicating trajectories behave more ballistically along ρ .

A. Acknowledgements

We thank J. Onuchic, I. Rips, N. Socci, and J. Wang for helpful discussions. This material is based upon work supported by the National Institutes of Health under award number PHS R01GM44557.

REFERENCES

- [1] J. Bryngelson and P. Wolynes, J Phys. Chem., **93**, 6902 (1989).
- [2] S. Plotkin, J. Wang and P. Wolynes, J Chem. Phys. , **106**, 2932 (1997).
- [3] N. Socci, J. Onuchic and P. Wolynes, J Chem. Phys.,**104**, 5860 (1996).
- [4] D. Klimov and D. Thirumalai, Phys. Rev. Lett., **79**, 317 (1997).
- [5] J. Onuchic, P. Wolynes, Z. Luthey-Schulten and N. Socci, Proc. Nat. Acad. Sci. USA, **92**, 3626 (1995).
- [6] R. Grote and J. Hynes, J Chem. Phys., **73**, 2715 (1980).
- [7] J. Onuchic and P. Wolynes, J Phys. Chem., **92**, 6495 (1988).
- [8] E. Pollak, S. Tucker and B. Berne, Phys. Rev. Lett., **65**, 1399 (1990).
- [9] A. Berezhkovskii, E. Pollak and V. Zitserman, J Chem. Phys., **97**, 2422 (1992).
- [10] E. Pollak, J Phys. Chem., **95**, 10235 (1991).
- [11] A.Šali, E. Shakhnovich and M. Karplus, Nature, **369**, 248 (1994).
- [12] E. Boczko and C. Brooks, Science, **269**, 393 (1995).
- [13] K. Dill and H. Chan, Nat. Struct. Biol., **4**, 10 (1997).
- [14] R. Du, V. Pande, A. Grosberg, T. Tanaka and E. Shakhnovich, (preprint), (1997).
- [15] J. Wang, S. Plotkin and P. Wolynes, J. Phys. I France, **7**, 395 (1997).
- [16] M. Shlesinger and E. Montroll, Proc. Nat. Acad. Sci. USA, **81**, 1280 (1984).
- [17] J-P. Bouchaud and D. Dean, J. Phys. I France, **5**, 265 (1995).
- [18] E. DiMarzio and I. Sanchez, in *Transport and Relaxation in Random Materials*, ed. J. Klafter, R. Rubin and M. Shlesinger (World Scientific, Singapore, 1986).
- [19] R. Zwanzig, J Stat. Phys., **9**, 215 (1973).
- [20] W. Miller, J Chem. Phys., **61**, 1823 (1974).
- [21] N. Socci, J. Onuchic, P. Wolynes, Proteins: Struct. Funct. and Genetics, (to appear) (1997).